



Deposited via The University of Sheffield.

White Rose Research Online URL for this paper:

<https://eprints.whiterose.ac.uk/id/eprint/142143/>

Version: Published Version

Article:

Totea, A.M., Dorin, I., Gavrilov, G. et al. (2019) Real time calorimetric characterisation of clay – drug complex dispersions and particles. *International Journal of Pharmaceutics: X*, 1. 100003. ISSN: 2590-1567

<https://doi.org/10.1016/j.ijpx.2018.100003>

Reuse

This article is distributed under the terms of the Creative Commons Attribution-NonCommercial-NoDerivs (CC BY-NC-ND) licence. This licence only allows you to download this work and share it with others as long as you credit the authors, but you can't change the article in any way or use it commercially. More information and the full terms of the licence here: <https://creativecommons.org/licenses/>

Takedown

If you consider content in White Rose Research Online to be in breach of UK law, please notify us by emailing eprints@whiterose.ac.uk including the URL of the record and the reason for the withdrawal request.



Real time calorimetric characterisation of clay – drug complex dispersions and particles



A.M. Totea^a, I. Dorin^b, G. Gavrilov^c, P.R. Laity^d, B.R. Conway^a, L. Waters^a, K. Asare-Addo^{a,*}

^a School of Applied Sciences, Department of Pharmacy, University of Huddersfield, Queensgate, Huddersfield HD1 3DH, UK

^b Malvern Panalytical Ltd., Malvern, UK

^c Wienerberger, Baneasa Business & Technology Park, Bucharest, Romania

^d Department of Materials Science and Engineering, University of Sheffield, Sir Robert Hadfield Building, Mappin Street, Sheffield S1 3JD, UK

ARTICLE INFO

Keywords:

Magnesium aluminium silicate
 Propranolol hydrochloride
 Isothermal titration calorimetry
 Complexation

ABSTRACT

Isothermal titration calorimetry (ITC) along with attenuated total reflectance Fourier transform infrared spectroscopy (ATR-FTIR), scanning electron microscopy with energy dispersive X-ray spectroscopy (SEM/EDX) and high-performance liquid chromatography (HPLC) were employed to investigate the process of adsorption of propranolol hydrochloride (PPN) onto magnesium aluminium silicate (MAS) and to characterise the MAS-PPN particles formed upon complexation. The composition of MAS was confirmed by infrared (IR) spectroscopy and a calcimeter. The calorimetric results confirmed the binding between PPN and MAS at various pHs and temperatures. The overall change in enthalpy was found to be exothermic with a comparatively small entropic contribution to the total change in Gibbs free energy. These findings suggest that the binding process was enthalpically driven and entropically unfavourable (lower affinity) suggesting hydrogen bonding and electrostatic interactions dominating the interaction. The variation of pH and temperature did not have a great impact on the thermodynamics of the binding process, as observed from the similarity in enthalpy (ΔH), entropy (ΔS) or Gibbs free energy (ΔG). A slight reduction in the binding affinity (K_a) with varying pH and temperature was however observed. SEM/EDX studies showed the occurrence of changes in the microstructural properties of MAS following complexation which may explain the potential of MAS-PPN complexes for controlled drug release promoting pharmaceutical innovation.

1. Introduction

Sustained-release drug formulation is of high importance as it achieves optimal therapeutic efficacy in chronic conditions where treatment must be administered at constant levels over a period of time, and provides a reduced frequency of side effects (Aulton, 2007). In recent years, excipients such as clay minerals have often been used as carriers of active ingredients to retard or modulate drug release (Trikeriotis and Ghanotakis, 2007; Park et al., 2008; Joshi et al., 2009; Meng et al., 2009; Pongjanyakul et al., 2009; Rojtanatanya and Pongjanyakul, 2010). Their physicochemical properties make them suitable to be used in the formulation of pharmaceutical dosage forms, as they can adsorb the active ingredient onto their structure and form complex dispersions and particles (Carretero and Pozo, 2009; Pongjanyakul et al., 2009; Rojtanatanya and Pongjanyakul, 2010;

Kanjanakawinkul et al., 2013; Rongthong et al., 2013). These have been shown to modify the release of drugs upon administration, which would be desirable for drugs having a short half-life and require frequent administration to maintain adequate drug plasma levels (Rojtanatanya and Pongjanyakul, 2010).

Magnesium aluminium silicate (MAS) used in this research is a mixture of natural smectite montmorillonite and saponite clays, often used to improve the physical characteristics of drugs and to control their release (Pongjanyakul et al., 2009; Kanjanakawinkul et al., 2013). MAS has a high surface area, a very good affinity with cationic drugs and it is neither toxic nor irritant, therefore being suitable to be used within drug formulation. MAS has a layered silicate structure, formed of one alumina or magnesia octahedral sheet, sandwiched between two tetrahedral silicate sheets (Fig. 1) (Kanjanakawinkul et al., 2013). Hydration in polar liquids easily allows the delamination of MAS platelets,

Abbreviations: MAS, magnesium aluminium silicate; PPN, propranolol hydrochloride; ITC, isothermal titration calorimetry; SIM, single injection mode; MIM, multiple injection mode; HPLC, high performance liquid chromatography; RSD, relative standard deviation; ICH, International Conference on Harmonisation; LOD, limit of detection; LOQ, limit of quantification; HCl, hydrochloric acid; rpm, rotations per minute

* Corresponding author.

E-mail address: k.asare-addo@hud.ac.uk (K. Asare-Addo).

<https://doi.org/10.1016/j.ijpx.2018.100003>

Received 30 October 2018; Received in revised form 13 December 2018; Accepted 15 December 2018

Available online 21 December 2018

2590-1567/ © 2018 The Author(s). Published by Elsevier B.V. This is an open access article under the CC BY-NC-ND license

(<http://creativecommons.org/licenses/by-nc-nd/4.0/>).

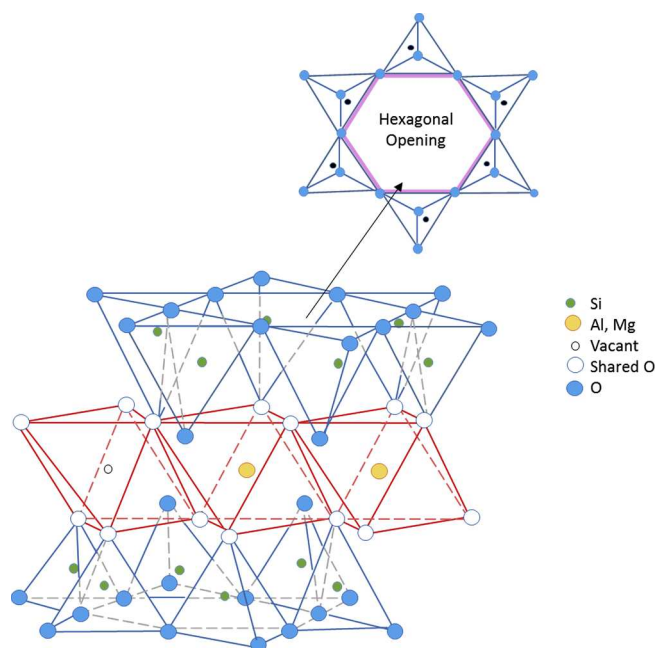


Fig. 1. Alumina or magnesia sheet composed of octahedron structures joined together and sandwiched between two silica sheets composed of silica tetrahedron structures joined together (adapted from (Vanderbilt Minerals, 2014b)).

which would otherwise be very difficult to achieve mechanically, due to the binding effect of counter ions and water found between platelets. Water easily forces the clay platelets further apart as it penetrates between them (osmosis) and hence cations diffuse away from platelet faces (diffusion) (Vanderbilt Minerals, 2014a,b). This allows the exposure of the negative face of the clay platelets which, in turn, allows the adsorption of cationic drugs via electrostatic interactions (Nunes et al., 2007; Pongjanyakul et al., 2009; Rojtanatanya and Pongjanyakul, 2010).

The present study investigates a potential clay-based formulation of a model cationic drug propranolol hydrochloride (PPN) selected on the basis of its important therapeutic effect but short half-life. PPN represents the first of drugs acting as antagonists at β -adrenergic receptors of the heart (β -blockers), developed in the 1960s and introduced in 1964 (Patrick, 2001; Rojtanatanya and Pongjanyakul, 2010). Its therapeutic effect comes from antagonizing the adrenergic pathway that can lead to blocking receptors in heart, lungs, liver, pancreas, peripheral blood vessels and other parts of the body. It is used to treat angina pectoris, myocardial infarction and high blood pressure. However, due to its high solubility in water, PPN has a short half-life of 3.9 h and hence, it needs to be administered frequently (2–3 times/day) in order to maintain adequate drug plasma levels (Datta, 2013). The development of sustained-release dosage forms would be beneficial, increasing patient compliance, safety and efficacy of the drug.

Here, the authors have studied the adsorption of PPN onto MAS using isothermal titration calorimetry (ITC), high performance liquid chromatography (HPLC), attenuated total reflectance Fourier transform infrared spectroscopy (ATR-FTIR) and scanning electron microscopy with energy dispersive X-ray spectroscopy (SEM/EDX).

Isothermal titration calorimetry (ITC) is the only technique able to completely characterise the thermodynamics of an interaction in a single experiment (MicroCal, 1998). ITC is a powerful well-established biophysical technique used to measure the formation and dissociation of molecular complexes in many branches of science from cell biology to food chemistry. ITC can be successfully used to study interactions using a wide variety of samples such as clays, polymers, metals, proteins, enzymes, hormones, antibodies and nanoparticles (Ladbury and Chowdhry, 1996; Penn and Warren, 2009; Le et al., 2013). Traditional

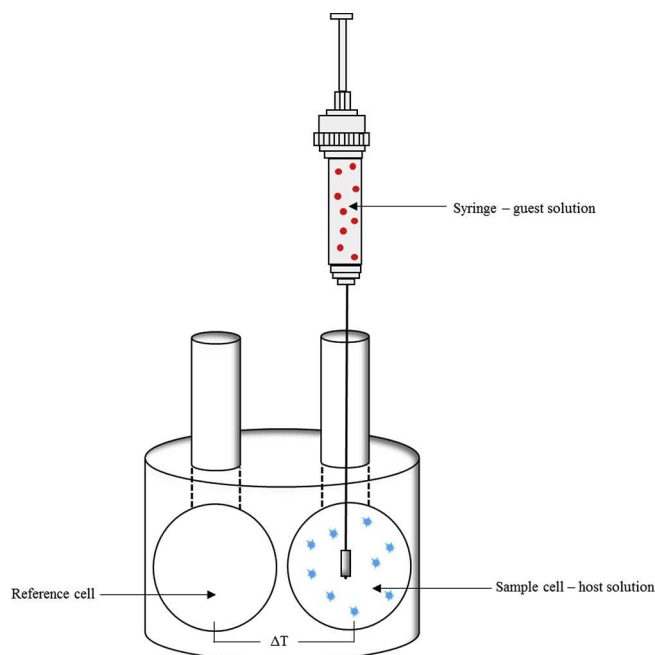


Fig. 2. Schematic diagram of an ITC micro calorimeter.

ITC experiments with multiple discrete injections have previously been used to provide accurate and important information about the mechanisms of binding of molecules (Callies and Hernández Daranas, 2016). Single injections experiments are faster and versatile, as the user can generate the binding isotherm in one third to half the time a multiple injection experiment takes, allowing the rapid determination of the suitable conditions and parameters for the reaction, as well as the driving forces for the reaction (Malvern Instruments, 2015). To perform an experiment, the instrument periodically injects a ligand (guest solution) into the calorimetric cell containing an analyte (host solution) under isothermal conditions (Fig. 2) (Duff et al., 2011). The heat absorbed or released as chemical bonds form or break is then measured as the power that must be supplied to maintain both sample and reference cells at a constant temperature (Moore et al., 2016; Di Trani et al., 2017). Experiments can be performed under different conditions, such as variable temperatures or buffer giving detailed information about the studied systems (Duff et al., 2011). Independent binding sites, sequential binding sites, competitive binding and dissociation models can be fitted to the resulting data to yield binding site size, affinity (K_a), changes in enthalpy (ΔH), entropy (ΔS) or Gibbs free energy (ΔG) and stoichiometry (N) of the binding events (Moore et al., 2016). For a simple single binding site model, the non-linear least squares fit of the data can be used to determine K_a and ΔH , followed by the calculation of ΔG and ΔS using the known relationship between the van't Hoff equation and change in Gibbs free energy:

$$\Delta G = \Delta H - T\Delta S \quad (1a)$$

$$= -RT \ln K_a \quad (1b)$$

where T is the absolute temperature in Kelvin and R is the gas constant.

The change in heat capacity of the binding interaction at constant pressure (ΔC_p) may also be determined by undertaking experiments at additional temperatures. ΔC_p is determined from the temperature dependence of ΔH using Eq. (2) (MicroCal, 1998; Le et al., 2013):

$$\Delta C_p = \frac{(\Delta H_{T_2} - \Delta H_{T_1})}{T_2 - T_1} \quad (2)$$

In certain cases, more complex models (with equilibria involving multiple binding mechanisms) are used to predict the thermodynamics

of the binding event (Le et al., 2013; Callies and Hernández Daranas, 2016). A spontaneous interaction will have a negative ΔG and, as the binding increases in strength, ΔG will also become increasingly negative. ΔG for a binding isotherm has both an entropic and an enthalpic contribution.

The present study aimed at exploiting ITC in giving insights to the binding that occurs in clays and model cationic drugs through the observation of the process in real time and determination of the driving forces that could potentially affect drug release. The real-time process of adsorption of cationic drugs onto clay minerals has not been described prior to this study and as such understanding it is a critical step in establishing a successful formulation thus promoting pharmaceutical innovation.

2. Experimental

2.1. Materials

VEEGUM F EP® (Magnesium Aluminium Silicate) was a gift from R.T.Vanderbilt Company, Norwalk, CT (USA). Its composition was confirmed by infrared (IR) spectroscopy and using a calcimeter. The calcimeter used works in accordance to the method of Scheibler which determines the carbonate content using a volumetric method (Calciometer Manual, 2018). The method involves the addition of hydrochloric acid to the clay sample which leads to the conversion of the carbonates into CO_2 . The amount of CO_2 released produces a difference in pressure which is measured on a burette filled with water and de-aerated. The difference in level on the burette is used to calculate the carbonate content as an equivalent calcium carbonate content. This material therefore complies with the European Pharmacopoeia monograph for Magnesium Aluminium Silicate and is indicated for use as a dry excipient in pressed powders and in direct compression tablets (Vanderbilt Minerals, 2014a). Propranolol hydrochloride was supplied from TCI (Tokyo Chemical Industry, Tokyo). Acetonitrile (HPLC grade), sodium phosphate dibasic dihydrate, 99 + % (HPLC grade), 2 M sodium hydroxide and 2 M hydrochloric acid were purchased from Fisher Scientific (UK).

2.2. Methods

2.2.1. Formulation of MAS-PPN complex particles

MAS dispersions (2% w/v) and PPN solutions (2% w/v) were separately prepared under continuous stirring at 500 rpm (25 °C) for 24 h and 30 min respectively. The pH of MAS dispersions and PPN solutions prepared was further adjusted to pH 5 using 2 M hydrochloric acid and 2 M sodium hydroxide. For single drug loading, one PPN solution was combined with one of the MAS dispersions prepared, and the obtained dispersion (1:1 w/w) was incubated at 37 °C with shaking at 200 rpm for 24 h (GLS Aqua 18 Plus, Linear Shaking Water Bath, Grant Instruments). The MAS-PPN complex dispersion formed was then filtered using a Buchner filtration apparatus with vacuum. For the second drug loading, previously filtered single drug loaded complexes prepared was redispersed into a fresh drug solution (at pH 5) and incubated at 37 °C with shaking at 200 rpm for 24 h. The single and double loaded MAS-PPN complex dispersions obtained were then filtered and dried in the oven at 50 °C for 48 h. The complexed particles obtained were ground using a Retsch® PM 100 Ball Mill set at 350 rpm. The ground samples were sieved to a particle size fraction of 123–65 μm and stored in a glass vial until needed.

2.2.2. Characterisation of MAS-PPN complexes

2.2.2.1. Attenuated total reflectance Fourier transform infrared spectroscopy (ATR-FTIR). ATR-FTIR was used to elucidate the molecular interaction between MAS and PPN. Experiments were performed on a Smart Orbit ATR-FTIR machine, using diamond as the ATR crystal. MAS, PPN and MAS-PPN complexes (dried single and

double drug loaded complexes) were scanned from 4000 to 400 cm^{-1} .

2.2.2.2. Scanning electron microscopy with energy dispersive X-ray spectroscopy (SEM/EDX). The surface morphology in 3D and the energy spectrum of samples was analysed using a QUANTA FEG 250 microscope equipped with an EDX to detect changes that occurred following the complexation process. The electronic beam voltage of the microscope was set at 20 kV. A small amount of either PPN, MAS or the single and double loaded MAS-PPN complexed samples was mounted on a metal stub with double-sided adhesive tape and sputter coated with a thin layer of gold (1–5 nm) under vacuum (argon atmosphere). Various magnifications were taken of the micrographs to aid in the study of the complexes.

2.2.3. Drug content analysis from single and double loaded MAS-PPN complexes

Drug content within the single and double loaded MAS-PPN complexes was determined by dispersing 50 mg of the prepared single or double drug loaded MAS-PPN complex particles in 100 mL of a 2 M HCl, ultra-pure water or pH 6.8 phosphate buffer under continuous stirring for 24 h, at 25 °C and 700 rpm. The suspensions obtained were then filtered using 0.2 μm syringe filters. The clear supernatant was analysed using HPLC (Section 2.2.4) to determine drug content in the MAS-PPN complexes. The experiments were performed in triplicate to ensure reproducibility.

2.2.4. High performance liquid chromatography (HPLC)

Reversed phase high performance liquid chromatography was performed using a Shimadzu HPLC system (Shimadzu, Japan), equipped with an SPD-20AV UV-Vis detector, using an XTerra® MS C18 150 mm \times 4.6 mm \times 3.5 μm column. The mobile phase was prepared using acetonitrile and 0.01 M sodium phosphate dibasic dihydrate (pH 3.5) at a ratio of 30:70 v/v. The flow rate of the mobile phase was set at 1 mL/min with a detection wavelength of 230 nm.

2.2.4.1. Method validation. The HPLC method used was validated by the following parameters: linearity range, precision, limit of quantitation (LOQ) and limit of detection (LOD) (Modamio et al., 1996). Linearity was evaluated over a series of drug stock solutions ranging from 100 to 0.1 $\mu\text{g/mL}$, prepared with appropriate volumes. A calibration graph was then generated by plotting the peak area versus the corresponding drug concentration ($R^2 \geq 0.999$). The results were recorded in triplicate on three different days. The intra and inter day precision was determined from an assay of freshly prepared 1, 10, 50 and 100 $\mu\text{g/mL}$ standard drug solutions, repeatedly run on the same day or on three different days. Results were evaluated statistically in terms of standard deviation (RSD %) (Ich, 2005). The intermediate and intra assay precision at three different concentration levels was lower than 2% RSD which complied with the acceptable criteria for quality control of pharmaceutical preparations (Ermer and Ploss, 2005; Chatpalliwar et al., 2012).

As a consequence of the basic nature of PPN, its analysis using HPLC was prone to peak tailing and poor peak shape from column overloading (McCalley, 2010; Sadeghi et al., 2013). Therefore, the sensitivity of the method is important in ensuring a good peak resolution and efficiency to avoid sample overloading (Sadeghi et al., 2013). The LOQ confirming the lowest drug concentration that can be recovered within acceptable limits of precision and accuracy was found to be 2.30 $\mu\text{g/mL}$, indicating the high sensitivity of the proposed method and its suitability for the detection of PPN in solution at low concentrations (Table 1). Furthermore, the LOD was determined to be 0.76 $\mu\text{g/mL}$ which also highlighted the sensitivity of the method.

2.2.5. Calorimetric binding studies

The VP-ITC instrument was calibrated to ensure its robustness, speed and ease of evaluation and to ensure the instrument was within

Table 1
HPLC method validation for PPN.

	Range ($\mu\text{g/mL}$)	Linearity (R^2)	Intermediate precision (RSD) (%)	Intra assay precision (RSD) (%)	LOD ($\mu\text{g/mL}$)	LOQ ($\mu\text{g/mL}$)
PPN	100–0.1	≥ 0.9998	1 $\mu\text{g/mL}$: 5.60 10 $\mu\text{g/mL}$: 1.04 50 $\mu\text{g/mL}$: 0.25 100 $\mu\text{g/mL}$: 0.33	1 $\mu\text{g/mL}$: 1.62 10 $\mu\text{g/mL}$: 0.55 50 $\mu\text{g/mL}$: 0.09 100 $\mu\text{g/mL}$: 0.61	0.76	2.30

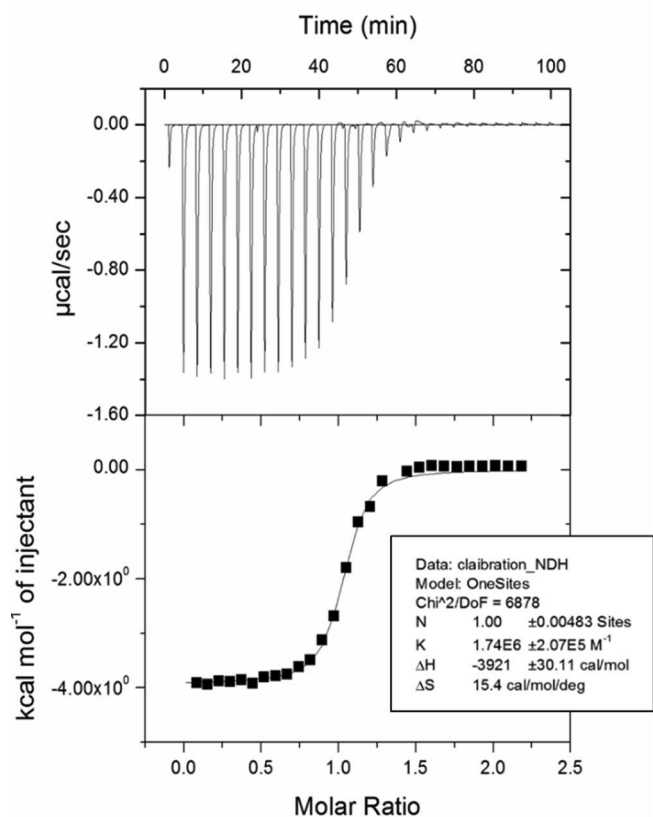


Fig. 3. Titration of 1 Mm CaCl_2 into 0.1 Mm EDTA solution at pH 6 (25 °C). Raw data (top) and integrated heats (bottom) as a function of molar ratio.

acceptable limits (Fig. 3) (Baranauskiene et al., 2009). Calorimetric binding studies were undertaken using a VP-ITC micro calorimeter (Malvern Analytical, UK) with the MAS dispersion in the sample cell and the PPN solution in the syringe. The instrument was used in high-gain feedback mode, applying a reference power of $20 \mu\text{cal s}^{-1}$ whilst stirring 307 rpm. The acidity of the working media (pH 5, 7, 9) in this study was chosen based on the pK_a value of PPN (9.5) (Shalaeva et al., 2007; Rojtanatanya and Pongjanyakul, 2010; ACD I-Lab, 2018). At these pHs, PPN is expected to be adsorbed onto the negatively charged MAS as it is ionised. 2 M hydrochloric acid and 2 M sodium hydroxide were used in adjusting the pH (ACD I-Lab, 2018). The results were analysed using Origin 7.0 (Microcal, Inc) software. Experiments were repeated in triplicate to ensure reproducibility.

Calorimetric single injection mode (SIM) binding studies were carried out at 25 °C and three different pH values, 5, 7 and 9 to characterise the process of adsorbing PPN onto MAS and to identify the most suitable conditions and parameters for the reaction. The drug solution was added as one 150 μL injection into the sample cell. MAS dispersions (0.037% w/v) and PPN solutions (0.150% w/v) were prepared using purified water under continuous stirring at 500 rpm (25 °C) for 24 h and 30 min respectively prior to analysis. The pH of the prepared solutions and dispersions was further adjusted to 5, 7 and 9. The binding isotherm was analysed by comparing the reaction rate for the adsorption

of PPN onto MAS at the pH values studied. Furthermore, the evolved heat in the experiments was analysed through a single set of sites curve fitting using a non-linear least squares model. This allowed the determination of the association constant K_a and the thermodynamic parameters ΔH , ΔG and ΔS .

Calorimetric multiple injection mode (MIM) binding studies were carried out at pH 5 and at two different temperatures (25 °C and 37 °C). The real-time binding isotherm was studied with 120 injections of 2 μL each into the sample cell every 260 s. MAS dispersion (0.037% w/v) and PPN solutions (0.150% w/v) were prepared as detailed previously.

3. Results and discussion

3.1. Chemical overview of MAS

The constituents of the MAS were confirmed to be a mixture of clay minerals and carbonates (Table 2). The high percentage of magnesia and alumina confirms the presence of both montmorillonite and saponite clays within the material (Table 2) (Kanjanakawinkul et al., 2013). Low quantities of ferric oxide, calcium oxide, potassium oxide and sodium oxide, as well as trace amounts of titanium oxide were observed, confirming the presence of exchangeable cations adsorbed onto the clay structure via electrostatic interactions. A loss on ignition of 11.90% resulted from the loss of water, organic matter and carbonates upon heating the sample between 120 and 150 °C (Weems, 1903). The MAS sample was further analysed by heating it to 900–1100 °C. This process produced 3.06% CO_2 which was a result of the thermal decomposition of the carbonates.

3.2. Solid state characterisation

3.2.1. Attenuated total reflectance Fourier transform infrared spectroscopy (ATR-FTIR)

ATR-FTIR was used to study the adsorption onto MAS of PPN based on the vibration of chemical bonds formed (Fig. 4). The spectrum of MAS alone indicated the presence of the hydroxyl group belonging to Si–OH at 3625 cm^{-1} and Si–O–Si stretching at 980 cm^{-1} (Rojtanatanya and Pongjanyakul, 2010). Also, a broad peak at 3415 cm^{-1} (O–H stretching of water residues) and a sharp peak at 1640 cm^{-1} (hydroxyl group bending of water of crystallization) were observed (Rojtanatanya and Pongjanyakul, 2010). The spectrum of PPN

Table 2

Chemical analysis of VEEGUM® F EP/ MAS confirming the amount of oxides and carbonates present in the sample as weight (%). Results obtained using IR spectroscopy and Calcmeter.

	Weight (%)		Weight (%)
Silica	58.63	Calcium carbonate	1.13
Ferric oxide	2.50	Magnesium carbonate	2.55
Alumina	11.91	Sodium carbonate	0.71
Calcium oxide	2.43	Potassium carbonate	2.55
Magnesia	7.69	Total	6.94
Sodium oxide	1.44		
Potassium oxide	3.26		
Titanium oxide	0.09		
Loss on ignition	11.90		
Total	99.85		

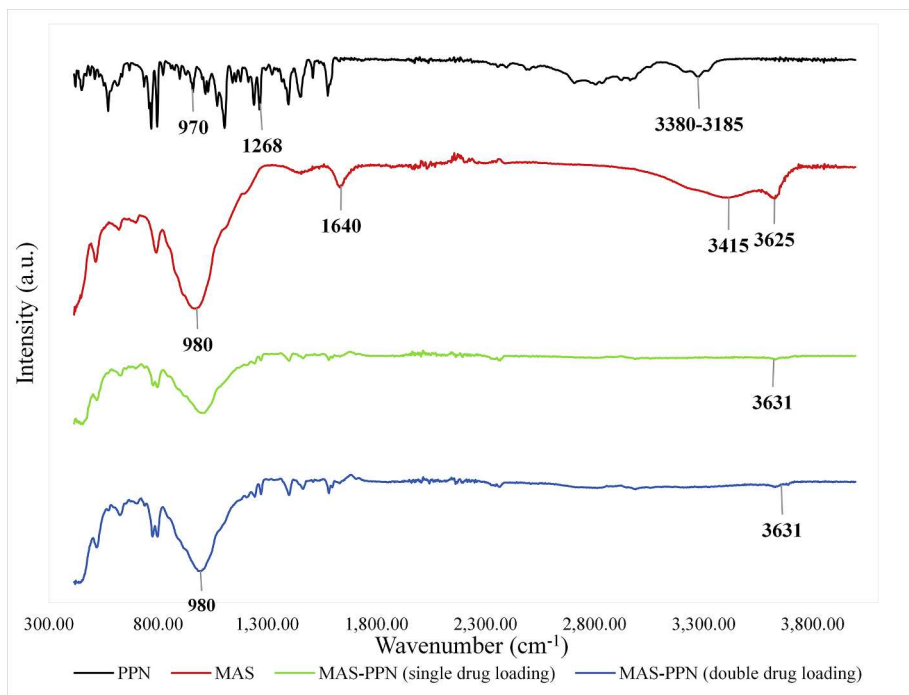


Fig. 4. ATR-FTIR spectra of PPN, MAS and single and double drug loaded MAS-PPN complex particles.

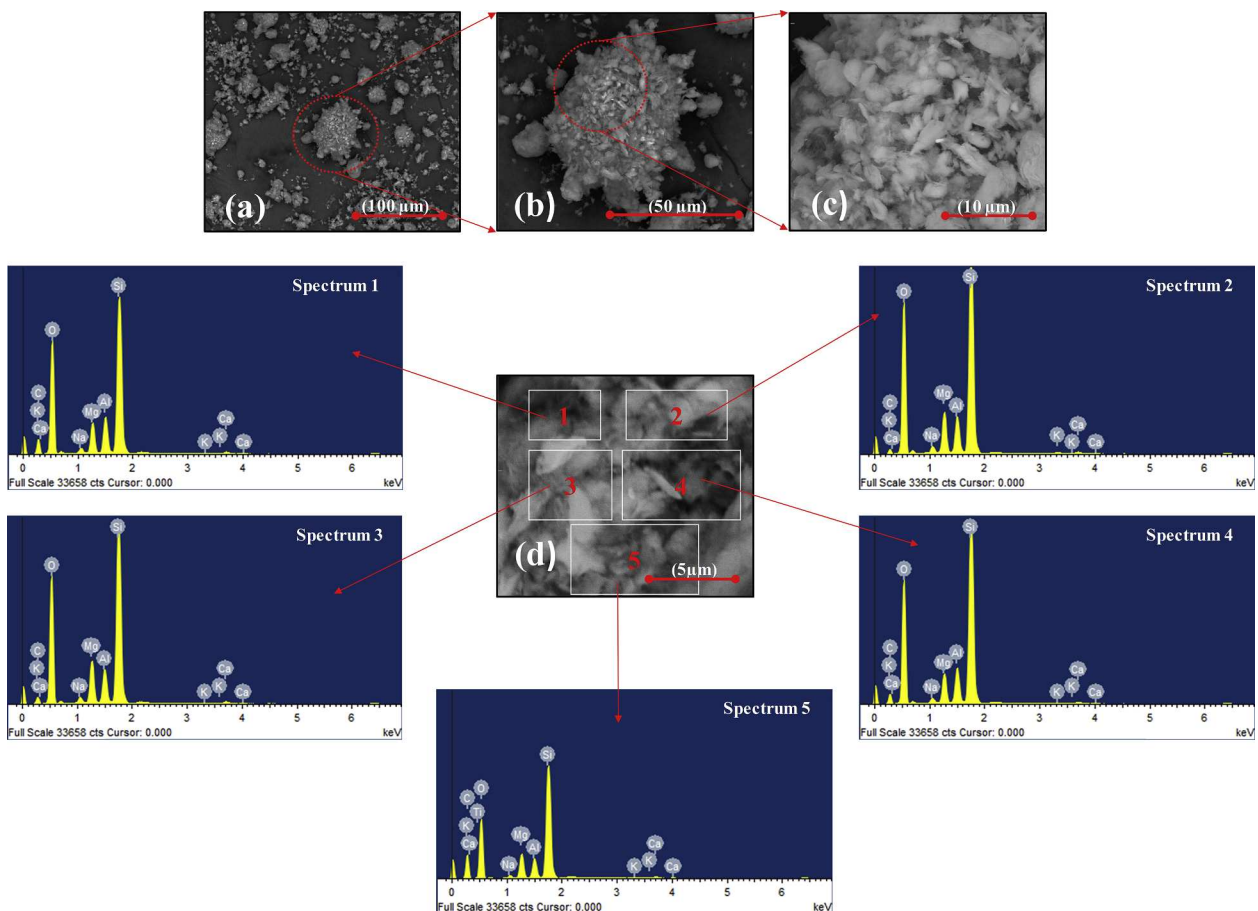


Fig. 5. Surface characterisation of MAS using SEM/EDX. SEM images at different magnifications $\times 500$ (a), $\times 1500$ (b), $\times 5000$ (c) and $\times 10,000$ (d); atomic distribution profile at five different sample locations (Spectrum 1–5).

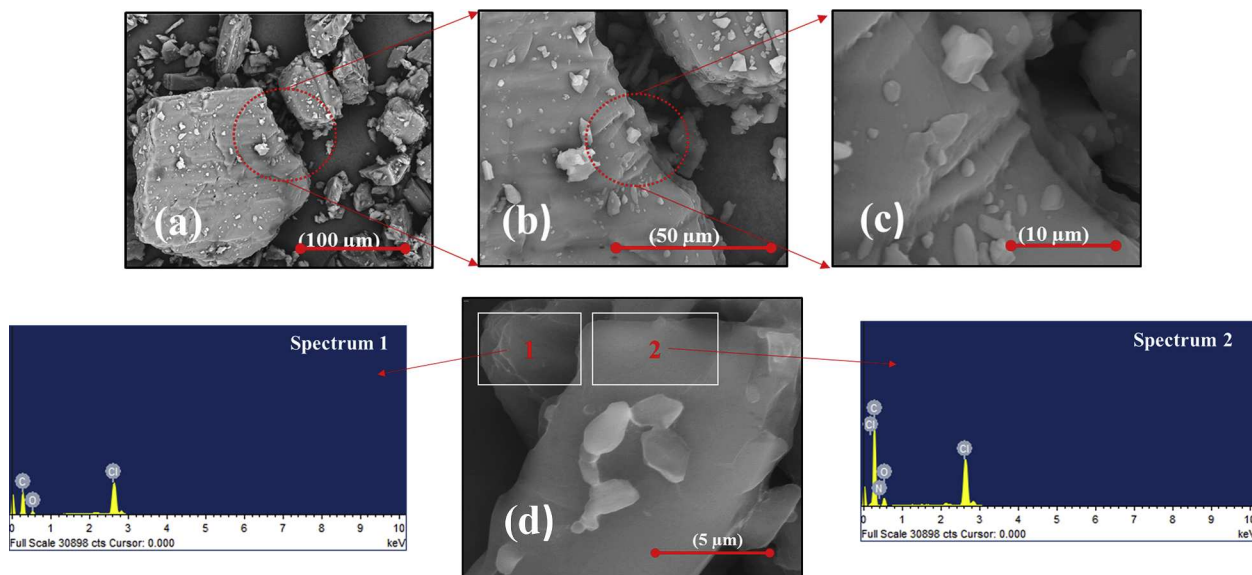


Fig. 6. Characterisation of PPN surface using SEM/EDX. SEM images at different magnifications $\times 500$ (a), $\times 1500$ (b), $\times 5000$ (c) and $\times 10,000$ (d); atomic distribution profile at two different sample locations (Spectrum 1 and 2).

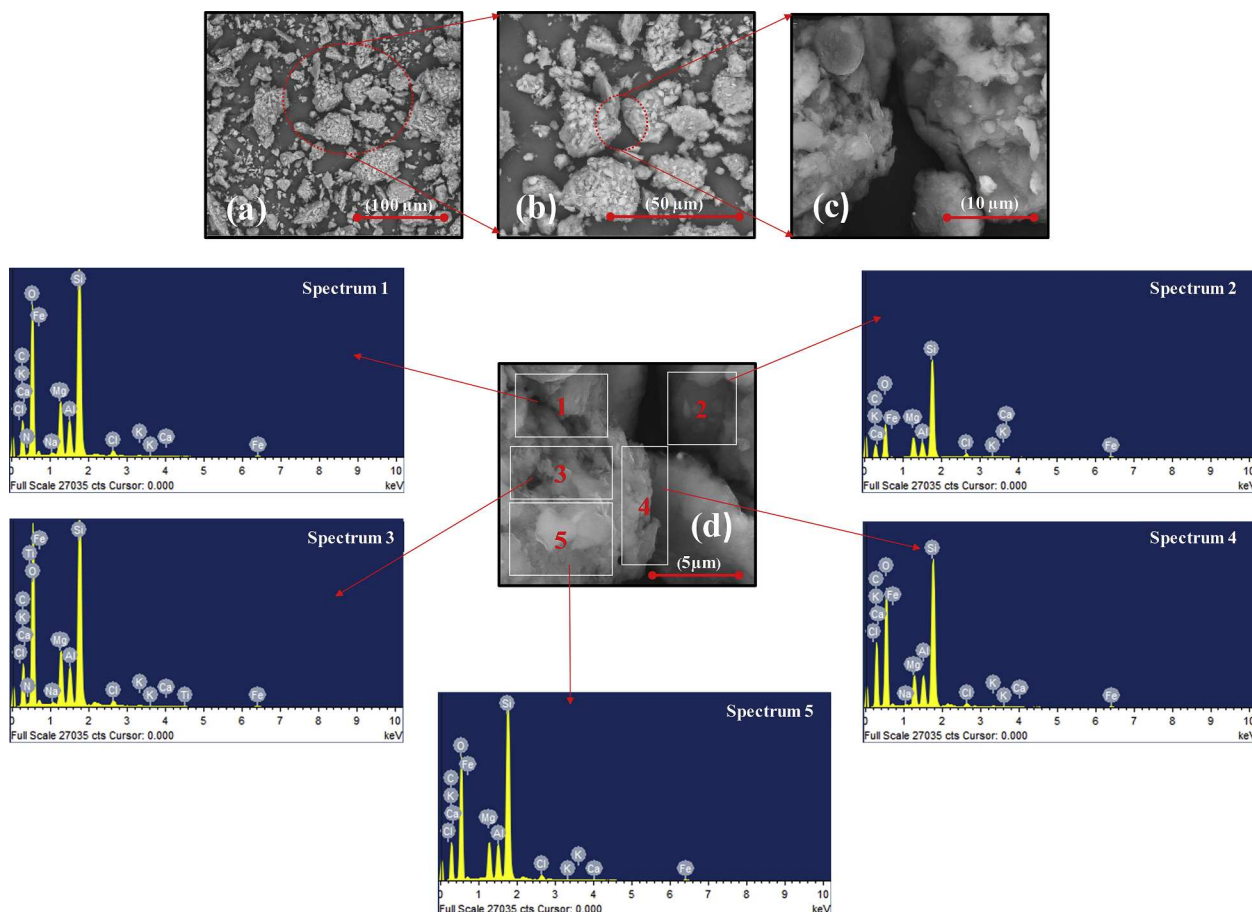


Fig. 7. Surface characterisation of MAS-PPN single drug loaded complex using SEM/EDX. SEM images at different magnifications $\times 500$ (a), $\times 1500$ (b), $\times 5000$ (c) and $\times 10,000$ (d); atomic distribution profile at five different sample locations (Spectrum 1–5).

alone displayed three distinctive peaks occurring between 3380 and 3185 cm^{-1} which can be attributed to the secondary hydroxyl and amine groups within its structure. The peak observed at 1268 cm^{-1} was attributed to aryl alkyl ether stretching, whilst the peak at 970 cm^{-1} was attributed to the naphthalene group within PPN (Rojtanatanya and

Pongjanyakul, 2010; Saeedi et al., 2013). Analysis of the single and double drug loaded MAS – PPN complexes displayed spectrums very different from the spectrum of PPN or MAS alone. The presence of the Si-O-Si stretching at 980 cm^{-1} from the clay was still observed, whereas the peak for the hydroxyl stretching of Si-OH became smaller and

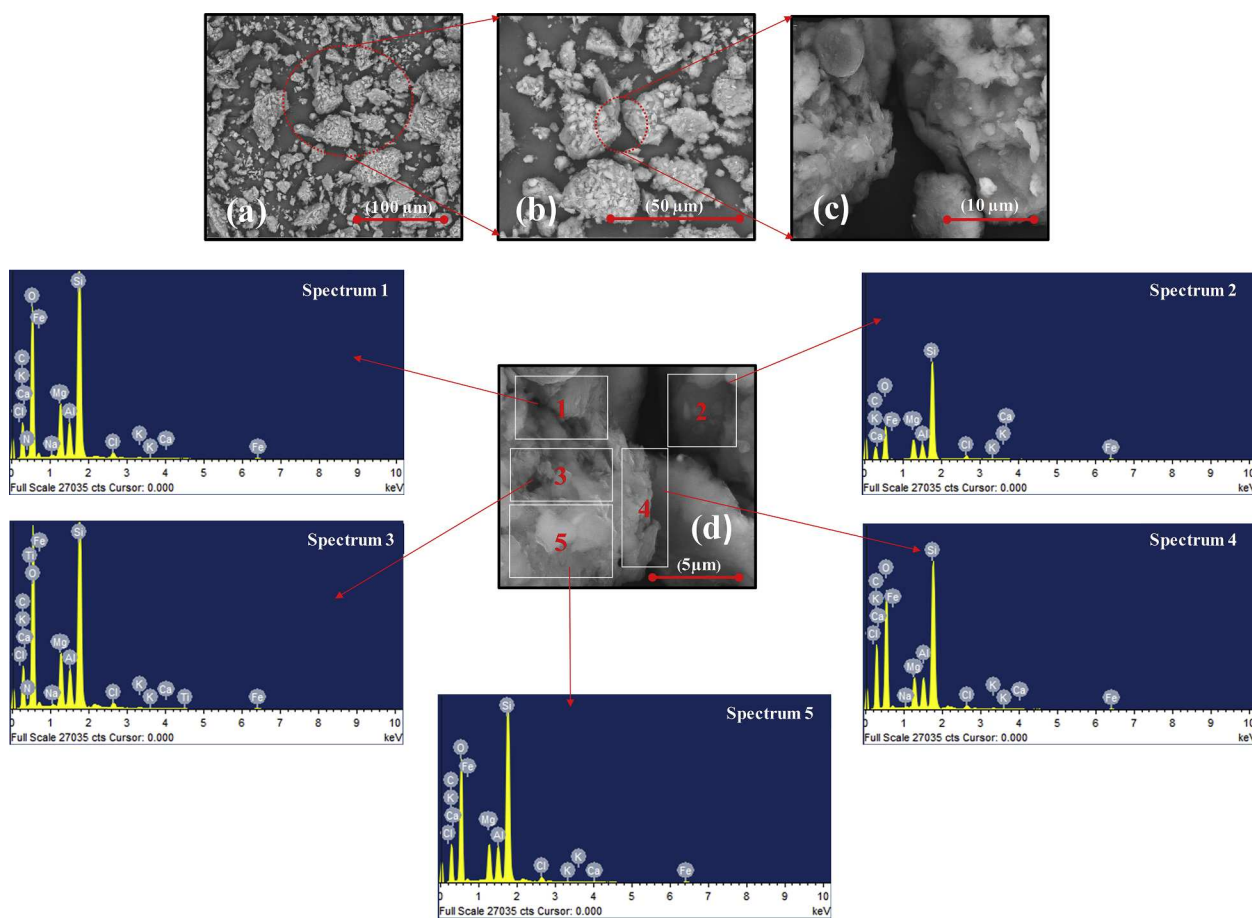


Fig. 8. Surface characterisation of MAS-PPN double drug loaded complex using SEM/EDX. SEM images at different magnifications $\times 500$ (a), $\times 1500$ (b), $\times 5000$ (c) and $\times 10,000$ (d); atomic distribution profile at five different sample locations (Spectrum 1–5).

Table 3

PPN content in single drug loaded and double drug loaded MAS-PPN complex particles using three different dissolution media (2 M HCl, ultra-pure water (pH 5) and phosphate buffer (pH 6.8)).

	Recovered PPN (% w/w)	
	MAS-PPN single drug loaded	MAS-PPN double drug loaded
2 M HCl	19.53 \pm 0.01*	25.94 \pm 0.42*
pH 5.0 Ultra-pure water	9.54 \pm 0.14*	16.09 \pm 0.57*
pH 6.8 Phosphate Buffer	12.61 \pm 0.18*	20.65 \pm 0.55*

Note: * values are reported as the mean \pm SD of at least three determinations.

shifted to a lower wavelength at approximately 3631 cm^{-1} . Peaks attributed to the secondary hydroxyl and amine groups within PPN were no longer visible. Hence, the change and disappearance of peaks from both MAS and PPN confirmed PPN adsorption onto MAS, via hydrogen bond formation between the silanol groups of MAS with the amine and/or hydroxyl groups of PPN (Rojtanatanya and Pongjanyakul, 2010).

3.2.2. Scanning electron microscopy with energy dispersive X-ray spectroscopy (SEM/EDX)

SEM images of the MAS particles were shown to be aggregated together in comparatively large clusters (Fig. 5) (Mita, Rupa and Achowicz, 2010; Pongjanyakul and Rojtanatanya, 2012). Individual flakes were also observed on the surface upon increasing magnification which represents the tetrahedral and octahedral sheets which are characteristic of phyllosilicates (Carrado and Bergaya, 2007). The atomic distribution onto the MAS surface using EDX revealed the

presence of high amounts of silicon, aluminium and magnesium, as well as trace amounts of iron, calcium, sodium, titanium and potassium (Fig. 5). The high percentage of silicon, magnesium and aluminium confirmed the presence of both montmorillonite and saponite clays within the material, whereas the other elements may indicate its provenience (Kanjankawinkul et al., 2013). The results were thus in agreement with that produced by the IR and calcimeter (Table 2). PPN was shown to be formed of large crystalline particles having smooth surfaces (Fig. 6). EDX analysis of PPN confirmed the presence of distinctive elements such as chlorine and nitrogen.

The analysis of the single and double drug loaded MAS-PPN complex particles using SEM/EDX (Figs. 7 & 8) indicated that both samples were similar, yet different when compared with MAS and PPN alone. These results indicate that changes in the microstructural properties of the clay powder occurred following the complexation process which may explain why the formed MAS-PPN complexes can be used to offer controlled drug release (Rojtanatanya and Pongjanyakul, 2010; Pongjanyakul and Rojtanatanya, 2012). The analysis of atomic distribution in the single and double drug loaded MAS-PPN complex particles revealed the presence of elements belonging to both PPN and MAS which was expected.

3.3. Recovery of PPN content from MAS-PPN complex particles

Drug recovery from the single and double drug loaded MAS-PPN complex particles was influenced by the dissolution media used (Table 3). A higher amount of PPN was recovered from the complexes in 2 M HCl and pH 6.8 buffer compared with ultra-pure water suggesting that the polydispersity of MAS particles was influenced by the

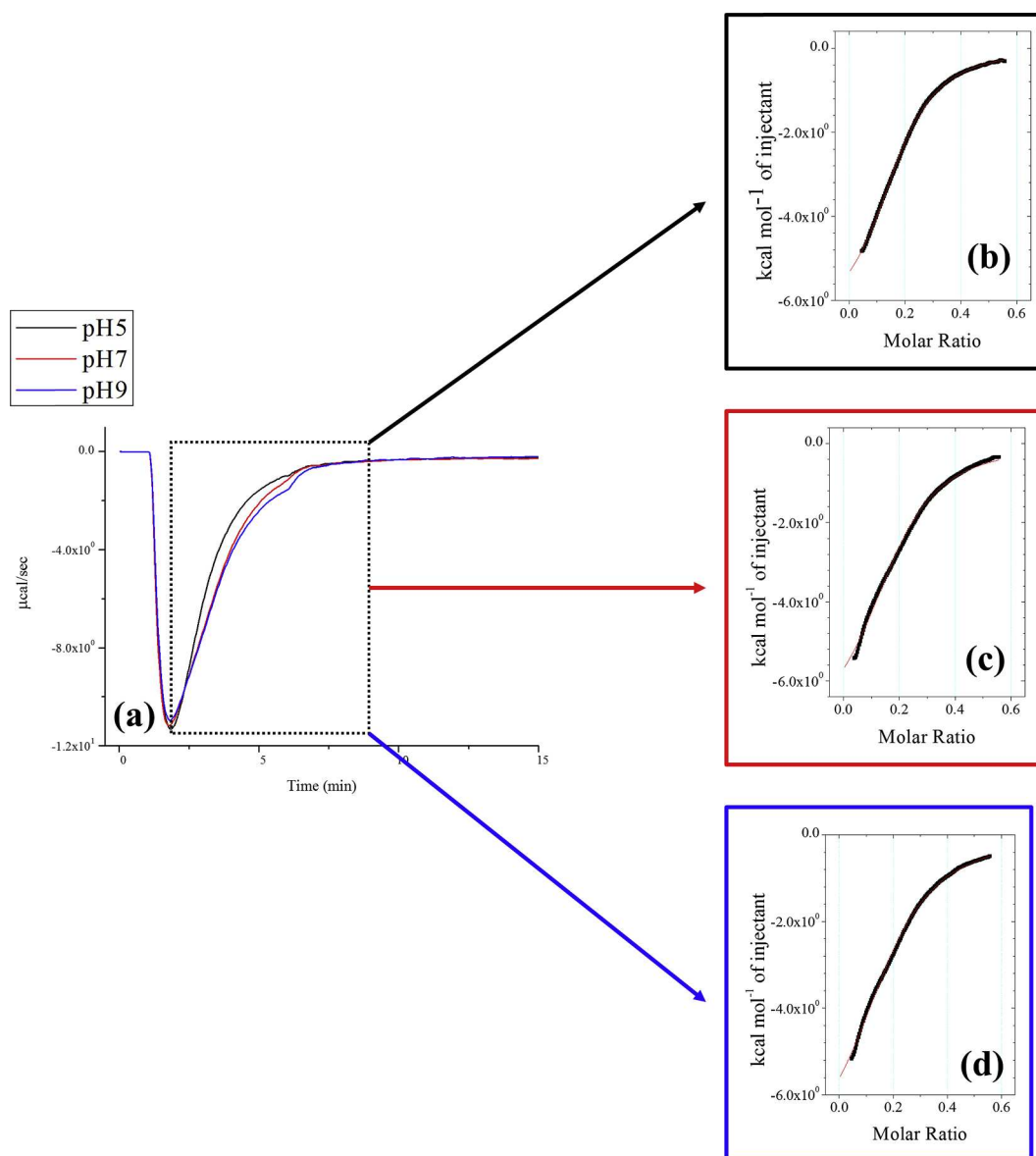


Fig. 9. SIM titration of PPN solution (0.150% w/v) into MAS dispersion (0.037% w/v) at pH 5 (black), pH 7 (red) and pH 9 (blue) (25 °C). The return to the baseline highlighted in purple is used to determine the most favourable (higher affinity) dissolution media for the interaction ($n = 3$) (a), data analysed through one set of sites curve fitting showing the enthalpy change (kcal mol^{-1} of injectant) at pH 5 (b), pH 7 (c) and pH 9 (d) all at 25 °C ($n = 3$). (For interpretation of the references to colour in this figure legend, the reader is referred to the web version of this article.)

Table 4

Calculated thermodynamic parameters using SIM calorimetric data regarding the adsorption of PPN (0.150% w/v) onto MAS (0.037% w/v) at pH 5, 7 and pH 9 (25 °C) ($n = 3$).

	pH 5	pH 7	pH 9
K_a	$2.22\text{E}+04 \pm 0.00$	$1.67\text{E}+04 \pm 1.91\text{E}+03$	$1.07\text{E}+04 \pm 2.52\text{E}+03$
ΔG			
kcal/mol	-5.46 ± 0.19	-5.48 ± 0.05	-5.87 ± 0.12
kJ/mol	-22.84 ± 0.79	-22.92 ± 0.21	-24.56 ± 0.50
ΔH			
kcal/mol	-7.62 ± 0.96	-7.33 ± 0.38	-8.20 ± 0.56
kJ/mol	-31.88 ± 4.02	-30.66 ± 1.59	-34.30 ± 2.34
$-\Delta S$			
kcal/mol/K	2.16 ± 0.71	1.85 ± 0.96	2.33 ± 1.76
kJ/mol/K	9.04 ± 2.97	7.74 ± 4.02	9.75 ± 7.36

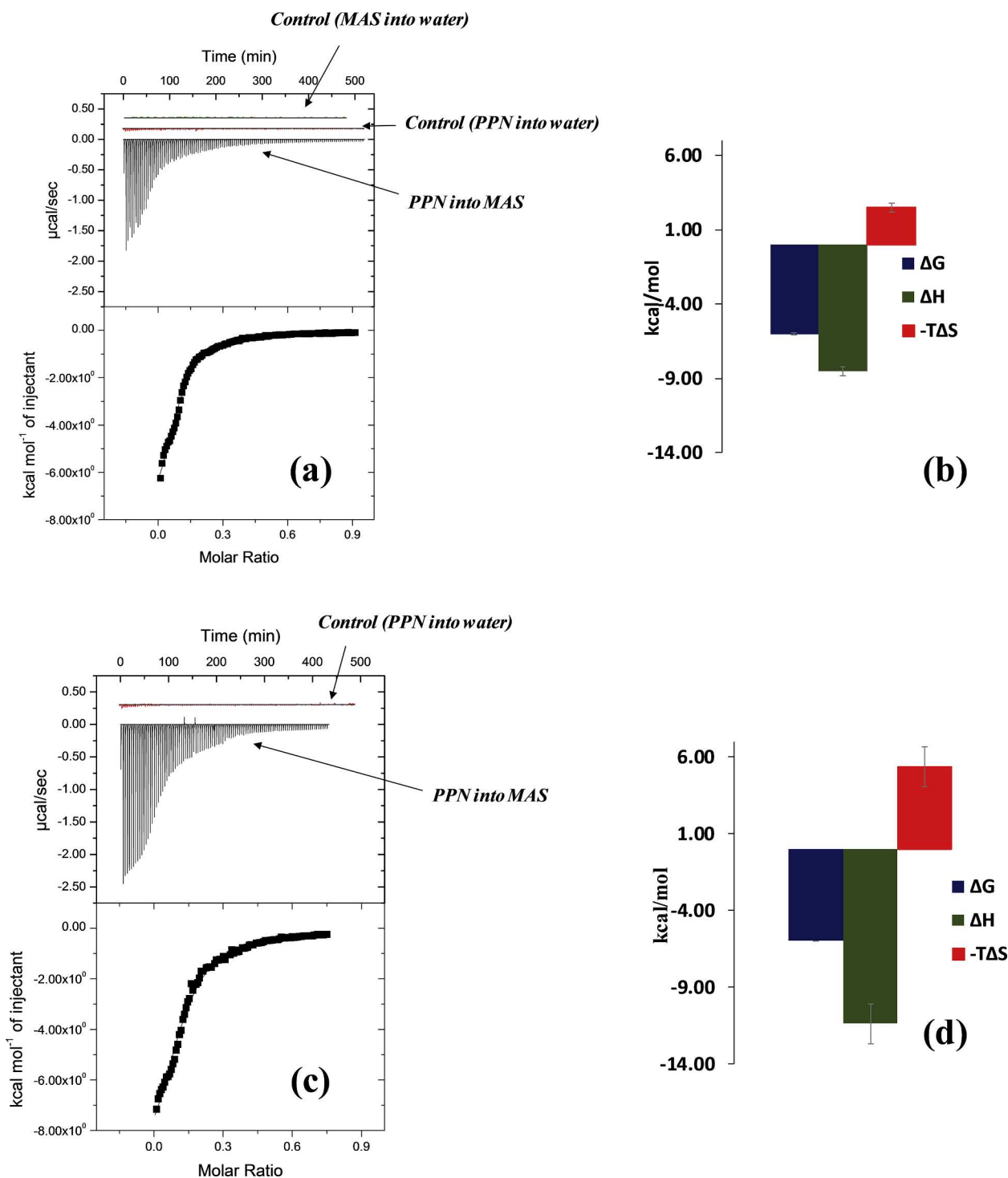


Fig. 10. An example of a multiple injection mode calorimetric titration of PPN solution (0.150% w/v, pH 5) into MAS dispersion (0.037% w/v, pH 5) at 25 °C. Raw data (top) and integrated heats (bottom) as a function of molar ratio (a), thermodynamic profile for binding of PPN onto MAS at 25 °C (b), multiple injection mode calorimetric titration of PPN solution (0.150% w/v, pH 5) into MAS dispersion (0.037% w/v, pH 5) at 37 °C. Raw data (top) and integrated heats (bottom) as a function of molar ratio (c) and thermodynamic profile for binding of PPN onto MAS at 37 °C (d).

cations present in the dissolution media (Rojtanatanya and Pongjanyakul, 2010). An increase in the PPN content was also observed in the MAS–PPN double drug loaded complexes suggesting that there were still available binding sites onto MAS after adsorption equilibrium was reached following the single drug loading which allowed further adsorption of PPN particles (Rojtanatanya and Pongjanyakul, 2010). It is key to note that no impurities or degradants were observed. This information is of high importance as it can affect the accurate

quantification of PPN from MAS–PPN complexes which, in turn, can impact on the formulation of a tablet dosage form.

3.4. Calorimetric binding studies

3.4.1. Single injection mode (SIM)

SIM experiments confirmed the adsorption of PPN onto MAS at the three pH values studied (pH 5, 7 and 9). This process was highly

exothermic and became more energetic as pH decreased, indicated by the peak returning more rapidly to the baseline (Fig. 9a). This can be attributed to the ionisation of the drug (pK_a 9.5) (Shalaeva et al., 2007; Rojtanatanya and Pongjanyakul, 2010; ACD I-Lab, 2018). It is important to note also that the MAS polydispersity may be affected by the ions in the solution which, in turn can affect the rate of adsorption of PPN onto MAS (Rojtanatanya and Pongjanyakul, 2010). SIM experiments through a single set of sites curve fitting using a non-linear least squares model allowed the observation of behaviour of adsorption of PPN onto MAS with varying pH (Fig. 9b–d and Table 4). In all cases, the overall change in enthalpy was found to be exothermic with a comparatively small entropic contribution to the total change in Gibbs free energy. These findings firstly imply that the binding phenomenon was predominantly enthalpically driven as high energy resulted from broken and created hydrogen bonds and electrostatic interactions. Secondly the similarity in values implies that pH did not affect the thermodynamics of the binding process. The binding affinity (K_a) slightly decreased with varying pH (Table 4) suggesting that at pH 5 the adsorption process was more energetic and the conditions for the reaction were optimum. The ITC data is thus in agreement with previous results published in literature showing that the adsorption of PPN onto MAS is enthalpically driven and entropically unfavourable suggesting hydrogen bonding and electrostatic interactions dominate the interaction (Rojtanatanya and Pongjanyakul, 2010; Pongjanyakul and Rojtanatanya, 2012).

3.4.2. Multiple injection mode

Multiple injection experiments at pH 5 and at two different temperatures (25 and 37 °C) further confirmed the highly exothermic interaction between PPN and MAS (Fig. 10), as observed in the SIM ITC experiments. The MIM stepwise experiments however gave detailed and more accurate information about the driving forces involved in the adsorption process compared with the SIM experiments. In agreement with previous SIM experiments, binding was characterised by a negative enthalpy change, and a comparatively small entropy change, i.e. implying that it was an enthalpically driven process (Fig. 10). The adsorption process of PPN onto MAS was shown to be similar at both 25 and 37 °C (Fig. 10b and d). The increase in temperature slightly decreased the affinity of PPN with MAS as observed from the reduction of the association constant K_a ($2.61E+04 \pm 2.71E+03$ M at 25 °C and $1.48E+04 \pm 1.48E+03$ M at 37 °C). The overall change in Gibbs free energy (ΔG) was comparatively similar at both temperatures (-6.03 ± 0.06 kcal/mol (-25.23 ± 0.25 kJ/mol) at 25 °C compared with -5.97 ± 1.37 kcal/mol (-24.98 ± 5.73 kJ) at 37 °C), confirming both reactions occurred spontaneously. The enthalpic contribution calculated from the change in heat associated with binding was greater at 37 °C (-11.37 ± 1.36 kcal/mol (47.57 ± 5.69 kJ) compared with -8.54 ± 0.32 kcal/mol (-35.73 ± 1.34 kJ) at 25 °C), while the entropic contribution was comparatively small in both cases confirming the interaction to be enthalpically driven at both temperatures. The binding interaction had a negative heat capacity ΔC_p (-0.24 kcal mol K^{-1} / -1.00 kJ mol K^{-1}) indicating that upon increasing temperature the binding became more exothermic and enthalpically driven, thus in agreement with the binding parameters calculated.

4. Conclusion

This study demonstrated the affinity of PPN for MAS and provided insights into its binding energetics. The process was shown to be exothermic, enthalpically driven and entropically unfavourable (lower affinity) suggesting hydrogen bonding and electrostatic interactions dominating the interaction. A simple, accurate and precise reversed-phase HPLC method was developed for quantitative determination of PPN from the single and double drug loaded MAS–PPN complex particles which showed that PPN recovery was influenced by the

dissolution media used, information which can impact on the formulation of a tablet dosage form. Changes in the microstructural properties of the clay powder following the complexation process were also observed which may explain why the formed MAS–PPN complexes could be used to offer controlled drug release strategies. ATR-FTIR confirmed PPN adsorption onto MAS, via hydrogen bond formation between the silanol groups of MAS with the amine and/or hydroxyl groups of PPN based on the vibration of chemical bonds formed. The detailed information presented in this study on the binding energetics and behaviour between PPN and MAS is of great importance to a formulator in the development of complexes for the manipulation of drug release.

Conflict of interest

The authors declare no conflict of interest.

Acknowledgements

Ana-Maria Totea thanks the University of Huddersfield for funding this project.

References

- ACD I-Lab (2018). Available at: <https://ilab.acdlabs.com/iLab2/> (Accessed: 23 September 2018).
- Aulton, M.E., 2007. *Aulton's Pharmaceutics*, third ed. Churchill Livingstone, Edinburgh.
- Baranauskienė, L., et al., 2009. Titration calorimetry standards and the precision of isothermal titration calorimetry data. *Int. J. Mol. Sci.* 10 (6), 2752–2762.
- CalciMeter Manual, 2018. Giesbeek. Eijkelkamp Soil & Water, Netherlands.
- Callies, O., Hernández Daranas, A., 2016. Application of isothermal titration calorimetry as a tool to study natural product interactions. *Nat. Prod. Rep.* 33 (7), 881–904.
- Carrado, K.A., Bergaya, F. (Eds.), 2007. *Clay-based Polymer Nano-composites (CPN)*. The Clay Minerals Society, Chantilly, VA, 20151-1125 Vol. 15.
- Carretero, M.I., Pozo, M., 2009. Clay and non-clay minerals in the pharmaceutical industry. Part I. Excipients and medical applications. *Appl. Clay Sci.* 46 (1), 73–80.
- Chatpalliwar, V.A., Porwal, P.K., Upmanyu, N., 2012. 'Validated gradient stability indicating HPLC method for determining diltiazem hydrochloride and related substances in bulk drug and novel tablet formulation'. *J. Pharmaceutical Anal. Xi'an Jiaotong Univ.* 2 (3), 226–237.
- Datta, S.M., 2013. Clay-polymer nanocomposites as a novel drug carrier: synthesis, characterization and controlled release study of propranolol hydrochloride. In: *Appl. Clay Sci.* 80–81. pp. 85–92.
- Duff Jr., M.R., Grubbs, J., Howell, E.E., 2011. Isothermal titration calorimetry for measuring macromolecule–ligand affinity. *J. Visualized Exp.* 55, 5–8.
- Ermer, J., Ploss, H.J., 2005. Validation in pharmaceutical analysis: Part II: Central importance of precision to establish acceptance criteria and for verifying and improving the quality of analytical data. *J. Pharm. Biomed. Anal.* 37 (5), 859–870.
- ICH, 2005. 'ICH Topic Q2 (R1) Validation of Analytical Procedures: Text and Methodology', International Conference on Harmonization, 1994 (November 1996), p. 17.
- Joshi, G.V., et al., 2009. Montmorillonite as a drug delivery system: intercalation and in vitro release of timolol maleate. *Int. J. Pharm.* 374 (1–2), 53–57.
- Kanjanakawinkul, W., et al., 2013. 'Nicotine-magnesium aluminum silicate microparticle surface modified with chitosan for mucosal delivery'. *Mater. Sci. Eng. C.* 33 (3), 1727–1736.
- Ladbury, J.E., Chowdhry, B.Z., 1996. Sensing the heat: the application of isothermal titration calorimetry to thermodynamic studies of biomolecular interactions. *Chem. Biol.* 3 (10), 791–801.
- Le, V.H., et al., 2013. Modeling complex equilibria in ITC experiments: thermodynamic parameters estimation for a three binding site model. *Anal. Biochem.* 434 (2), 233–241.
- Malvern Instruments, 2015. *Single Injection Method Software for MicroCal™ VP-ITC system*. Malvern.
- McCalley, D.V., 2010. The challenges of the analysis of basic compounds by high performance liquid chromatography: some possible approaches for improved separations. *J. Chromatogr. A* 1217 (6), 858–880.
- Meng, N., et al., 2009. Controlled release and antibacterial activity chlorhexidine acetate (CA) intercalated in montmorillonite. *Int. J. Pharm.* 382 (1–2), 45–49.
- MicroCal, 1998. *VP-ITC User's Manual*. Northampton.
- Mita, A.R.A., Rupa, A.K., Achowicz, R.J., 2010. Preliminary Approach to Application of Modified Smectite Clay to Form Tablets in Direct Compression Process, pp. 366–368.
- Modamio, P., et al., 1996. Development and validation of liquid chromatography methods for the quantitation of propranolol, metoprolol, atenolol and bisoprolol: application in solution stability studies. *Int. J. Pharm.* 130 (1), 137–140.
- Moore, D.E., et al., 2016. Isothermal titration calorimetry can provide critical thinking opportunities. *J. Chem. Educ.* 93 (2), 304–310.
- Nunes, C.D., et al., 2007. Loading and delivery of sertraline using inorganic micro and

- mesoporous materials. *Eur. J. Pharm. Biopharm.* 66 (3), 357–365.
- Park, J.K., et al., 2008. Controlled release of donepezil intercalated in smectite clays. *Int. J. Pharm.* 359 (1–2), 198–204.
- Patrick, G., 2001. *Medicinal Chemistry*. BIOS Scientific Publishers Limited, Oxford, UK.
- Penn, C.J., Warren, J.G., 2009. Investigating phosphorus sorption onto kaolinite using isothermal titration calorimetry. *Soil Sci. Soc. Am. J.* 73 (2), 560.
- Pongjanyakul, T., Khunawattanakul, W., Puttipatkhachorn, S., 2009. Physicochemical characterizations and release studies of nicotine-magnesium aluminum silicate complexes. *Appl. Clay Sci.* 44 (3–4), 242–250.
- Pongjanyakul, T., Rojtanatanya, S., 2012. Use of propranolol-magnesium aluminum silicate intercalated complexes as drug reservoirs in polymeric matrix tablets. *Indian J. Pharm. Sci.* 74 (4), 292–301.
- Rojtanatanya, S., Pongjanyakul, T., 2010. Propranolol-magnesium aluminum silicate complex dispersions and particles: characterization and factors influencing drug release. *Int. J. Pharm.* 383 (1–2), 106–115.
- Rongthong, T., et al., 2013. Quaternary polymethacrylate-magnesium aluminum silicate films: molecular interactions, mechanical properties and tackiness. *Int. J. Pharm.* 458 (1), 57–64.
- Sadeghi, F., et al., 2013. Validation and uncertainty estimation of an ecofriendly and stability-indicating hplc method for determination of diltiazem in pharmaceutical preparations. *J. Anal. Methods Chem.*
- Saeedi, M., Morteza-Semnani, K., Sagheb-Doust, M., 2013. Evaluation of *Plantago major* L. seed mucilage as a rate controlling matrix for sustained release of propranolol hydrochloride. *Acta Pharm.* 63 (1), 99–114.
- Shalaeva, M., et al., 2007. Measurement of dissociation constants (pKa Values) of organic compounds by multiplexed capillary electrophoresis using aqueous and cosolvent buffers. *J. Pharm. Sci.* 1–24.
- Di Trani, J.M., Moitessier, N., Mittermaier, A.K., 2017. Measuring rapid time-scale reaction kinetics using isothermal titration calorimetry. *Anal. Chem.* 89 (13), 7022–7030.
- Trikeriotis, M., Ghanotakis, D.F., 2007. Intercalation of hydrophilic and hydrophobic antibiotics in layered double hydroxides. *Int. J. Pharm.* 332 (1–2), 176–184.
- Vanderbilt Minerals, 2014a. VEEGUM / VAN GEL Magnesium Aluminum Silicate Magnesium Aluminum Silicate * The Story. Norwalk.
- Vanderbilt Minerals, 2014b. VEEGUM * Magnesium Aluminum Silicate VANATURAL * Bentonite Clay For Personal Care and Pharmaceuticals What They Are, pp. 1–27.
- Weems, J.B., 1903. *Chemistry of Clays*, Iowa Geological Survey Annual Report, 14(15), pp. 319–346.